SOLAR RADIO MICROBURSTS

T. S. Bastian
National Radio Astronomy Observatory
P. O. Box 0, Socorro, NM 87801

ABSTRACT

The Very Large Array was used for a period of ≈ 80 min on 1989 September 11 to observe the Sun at two frequencies in the 1.4 GHz band. In addition to a large flare, a multitude of small-amplitude, transient bursts occurred during the course of the observation. Specifically, > 11 transient radio enhancements occurred during a period of 65 min, ranging in amplitude from 0.07 – 4 sfu. These microbursts occurred at five distinct locations in four different active regions. The majority of the microbursts are probably due to plasma radiation although the detailed nature of the microburst mechanism remains unknown. Their relation to known radio burst phenomena and hard X-ray microflares is unclear.

I. INTRODUCTION

Microflares are of interest because of their possible bearing on the problems of coronal heating and solar flares. Microflares were first discovered as transient, small-amplitude hard X-ray (HXR) events by a sensitive, balloon-borne spectrometer flown on 1980 June 27 (Lin *et al.* 1984). The microflares occurred at a rate of roughly one every 5 min and ranged in duration from a few seconds to ~ 20 s. Several HXR microflares were found to be well-fit by a single power-law; hence HXR microflares are fundamentally nonthermal in nature. Lin *et al.* found that the integral number of HXR microflares increased with decreasing flux; on this basis, Lin *et al.* concluded that HXR microflares may be energetically significant and, possibly, of importance to the problem of coronal heating.

Microflares have not been studied in detail at radio wavelengths. However, there is good reason to believe that microflares are accompanied by radio emission; the correlation between radio emissions of various kinds and hard X-ray emission is well-known. Kundu (1961) first pointed out the close correlation between microwave bursts and HXR emission; Kane (1972) showed the existence of a correlation between type III bursts at meter wavelengths and impulsive HXR emission. More recently, correlations have been found between HXR bursts and decimetric (dm) phenomena including "blips" (Benz *et al.* 1983), type IIIdm bursts (Aschwanden *et al.* 1985), millisecond spikes (Benz 1986), and quasi-periodic pulsations (Aschwanden *et al.* 1990a).

In this poster I show that the Very Large Array (VLA) is ideally suited to explore the question of very weak solar radio emissions. It was recently used to detect a multitude of small-amplitude, transient, radio enhancements which occurred on an almost continuous basis at five distinct locations in four different active regions. I refer to these enhancements as *microbursts*. In Section II I describe the observational setup, present the microburst observations, and summarize their properties. In Section III I compare the observed properties of these microburst to burst phenomena at meter and decimeter wavelengths and discuss their bearing on the question of Hα and HXR microflares.

II. OBSERVATIONS

A. Observational Setup

The VLA was used on 1989 September 11 from 1850 – 2020 UT to image the full disk of the Sun in the 1.4 GHz band ($\lambda \approx 21$ cm). The 4 IF system used by the VLA made it possible to obtain simultaneous observations at 1446 and 1496 MHz in both senses of circular polarization. A bandwidth of 6.25 MHz was used for each IF. The observations were made using an integration time of 10 s; hence a snapshot image of the evolving radio emission was possible at each frequency and in each sense of circular polarization every 10 s. The array was in the C configuration in which 25 of 27 antennas were operable. The angular resolution of the snapshot images was approximately 12.5″ EW by 14.5″ NS for the Sun's declination of $\approx 4°$. The visibility data were calibrated using the AIPS calibration software. 3C286 was used as the flux and phase calibrator. The system temperature correction was applied offline.

B. Data Reduction and Analysis

The microbursts were first identified as shortterm enhancements in the fringe visibility amplitudes. Their appearance was even more striking after the visibility data were passed through a gradient filter. Fig. 1 shows the result for the 1496 MHz data as a function of baseline length and time; the microbursts appear as horizontal stripes. Note that both the rise and decay of the microbursts appear as positive in Fig. 1. In order to map the microwave burst sources, the time of the burst was identified and the pre-burst visibilities were vector subtracted from the data; in other words, an approximate baseline subtraction was performed. So long as the duration of the microburst was sufficiently short (some 10s of seconds), the error in the baseline determination was of the same order as the errors in the visibility measurements themselves. The microbursts were then mapped for each 10 s integration, CLEANed, and data cubes formed. The time profile of each burst was then determined by integrating the total flux over the source for each time stamp. Some examples are shown in Fig. 2a-c.

C. Observed Properties of the 1.4 GHz Microbursts

The locations of those active regions producing radio microbursts in the 1.4 GHz band are shown in Fig. 3. In Fig. 3a the KPNO magnetogram identifies those areas shown in detail in Fig. 3b-e. It was found that all enhancements could be attributed to five different sources in four different active regions. The properties of eleven microbursts are summarized in Table I although many more are apparent in Fig. 1. The observed properties of the microbursts may be summarized as follows:

- *All of the microbursts are spatially resolved, although some only slightly.*
- *The microburst amplitudes span almost orders of magnitude, ranging from 0.07 to 4 sfu. The inferred range of peak brightness temperature runs from 2 to 20 × 10^6 K.*
- *Four of the five microburst sources produced microbursts which were 100% circularly polarized. Two of the five produced moderately circularly polarized microbursts. All microbursts are polarized in the sense of the* ordinary *mode except, possibly, for event 9. Many of the microbursts are clearly associated with the lead sunspot of the active region in which they occur.*
- *The values of α vary widely, from -5 to +30, indicating that the bursts are at times narrow-band.*

The conditions required for microburst activity are unclear. All microburst activity occurred in active regions. One active region (No. 5683) showed subflare activity which was accompanied by microbursts (events 4 and 5). Significant microburst activity was also observed in active region No. 5680 following the impulsive phase of a large flare there (Bastian 1990). Active region Nos. 5676 and 5683 showed subflare activity within ±3 hrs of the observed microburst activity. On the other hand, active region No. 5689 produced persistent microburst activity but no flares until 36 hours later. Conversely, subflare and C-class flare activity was reported in several other active regions (e.g. Nos. 5669, 5682, 5687, and 5690) within ±6 hrs of the VLA observation, yet no microburst activity was seen in these active regions.

III. DISCUSSION

The most likely emission mechanism for most of the observed microbursts is plasma radiation at the local electron plasma frequency or its harmonic. It can account for the the high degree of circular polarization associated with many of the events and the fact that all but one are in the sense of the ordinary mode. The possibility that event 10 may instead be due to cyclotron or gyrosynchrotron emission cannot be excluded. I assume for the purposes of discussion, however, that most of the observed microbursts were due to plasma radiation at the fundamental or harmonic of the local plasma frequency; the corresponding electron number density in source is 2.8×10^{10} cm^{-3} in the former case, or 7×10^{9} cm^{-3} in the latter.

Because of the poor temporal and spectral resolution inherent to the observations, the burst mechanism cannot be identified with certainty. One possibility is that the microbursts are type III-like in character, resulting from discrete beams of nonthermal electrons propagating along the magnetic field in the low corona. In this respect, they may represent the decimetric analog to the microbursts identified at meter and dekameter wavelengths by Kundu *et al.* (1986) which presumably originated much higher in the solar corona. Consistent with this possibility are the low apparent brightness temperatures associated with the 1.4 GHz microbursts, a feature of meter-wave microbursts noted by Kundu *et al.* and discussed in detail by White *et al.* (1986) and Thejappa *et al.* (1990). The sense of polarization of type III bursts is believed to correspond to the ordinary mode. Usually, the polarity of the magnetic field deduced from the type III polarization measurements corresponds to that of the leading spot in the active region in which they occur (Dulk and Suzuki 1980). Typical durations of type III bursts near 1 GHz are a few times 0.1 s. To account for the present observations it must be assumed that a given 1.4 GHz microburst is in fact composed of tens or hundreds of small-amplitude type III-like bursts which appear as a longer duration event due to instrumental averaging. If this is the case, the inferred brightness temperatures represent weak lower limits.

Alternatively, the 1.4 GHz microbursts might be identified with the decimetric "blips", first discovered between 600 and 1000 MHz (Benz *et al.* 1981; Fürst *et al.* 1982; Benz *et al.* 1983). Blips are believed to be type III-like bursts although, in contrast to type III bursts, they are are narrowband ($\approx$30 MHz) of somewhat shorter duration ($\lesssim$0.2 s), and tend to occur in larger groups than type III bursts. Benz *et al.* (1983) show that blips show a higher degree of correlation with HXR bursts than do type III bursts. Again, the poor temporal and spectral resolution of the VLA observations preclude positive identification of the microbursts as blips. Note, however, that the broad range of values observed for α indicates the presence of discrete, narrow-band emissions, distributed over at least 50 MHz in bandwidth (the separation of the two frequencies sampled).

One property of many of the 1.4 GHz microbursts that stands in marked contrast to type III bursts and blips is the degree of polarization. Blips and fundamental Type III bursts tend to show low to moderate degrees of circular polarization while many of the microbursts show extremely high degrees of circular polarization. However, fundamental type III bursts are expected to be 100% circularly polarized and it is widely believed that the low to moderate degrees of circular polarization observed are due to a depolarizing mechanism which acts on the radiation as it traverses the corona. Zheleznyakov and Zlotnik (1964) developed the theory of depolarization in quasi-trasverse (QT) regions wherein significant depolarization occurs when the frequency of the emitted radiation is of the same order of a transition frequency ν_t, with

$$\nu_t^4 = \frac{\pi}{2}\frac{\nu_p^2\nu_B^3}{c\lambda}$$

where ν_p is the electron plasma frequency, ν_B is the electron gyrofrequency, c is the speed of light, and λ is the rate per unit distance that the magnetic field direction changes relative to the ray path. With ν_p fixed by assumption, assuming a magnetic field strength of $\gtrsim$100 G, and taking $\lambda^{-1} = 10^4$ km one finds that ν_t exceeds 40 GHz. Hence, in the present case, one might suppose that the radiation is weakly mode-coupled and that depolarization in QT regions overlying the source is inoperative.

Alternatively, it is possible that the 1.4 GHz microbursts are unrelated to type III

11 September 1989

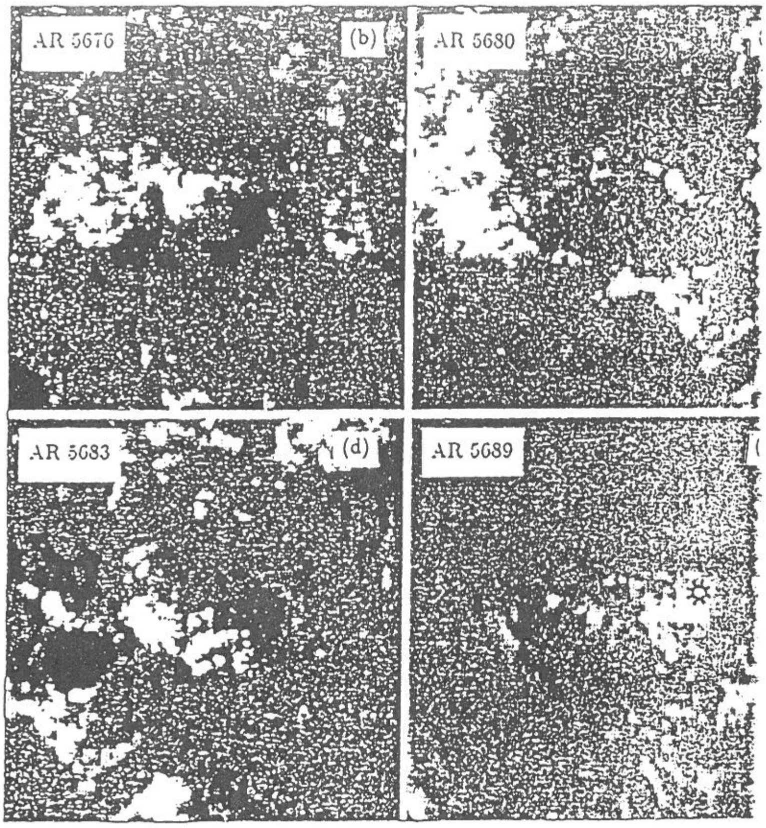

Figure 3

bursts or any of the other well-known bursts studied at meter and decimeter wavelengths. Previous observations have been made with relatively low sensitivity (tens of sfu); radio bursts had to be rather intense to be observed at all. In the present case, the burst activity is exceedly weak. Radio burst phenomena at these low amplitudes have not yet been explored.

The relation of the 1.4 GHz microbursts to microflares is therefore unclear. If the 1.4 GHz microbursts are indeed type III-like, i.e., are due to beams of nonthermal electrons, a close association of the microbursts with the HXR microflares reported by Lin *et al.* (1984) and/or Hα microflares (Canfield and Metcalf 1987) is likely. As such, they can be used as a sensitive indicator of discrete electron acceleration events in the solar active regions. If the microbursts are due to an entirely different mechanism, their relation to HXR and Hα microflare emission can only be clarified through further observations and an identification of the relevant microburst emission mechanism(s).

REFERENCES

Aschwanden, M. J., Wiehl, H. J., and Benz, A. O. 1985, *Solar Phys.*, 97, 159.

Aschwanden, M. J., Benz, A. O., Kane, S. R. 1990, *Solar Phys.*, 229, 206.

Bastian, T. S. 1991, in preparation.

Benz, A. O., Fürst, E., Hirth, W., and Perrenoud, M. R. 1981, *Nature*, 291, 239.

Benz, A. O. 1986, *Solar Phys.*, 96, 357.

Benz, A. O., Bernold, T. E. X., and Dennis, B. R. 1983, *Ap. J.*, 271, 355.

Canfield, R. C., and Metcalf, T. R. 1987, *Ap. J.*, 321, 586.

Dulk, G. A., and Suzuki, S. 1980, *Astr. Ap.*, 88, 203.

Fürst, E., Benz, A. O., and Hirth, W. 1982, *Astr. Ap.*, 107, 178.

Kane, S. R. 1972, *Solar Phys.*, 27, 174.

Kundu, M. R. 1961, *J. Geophys. Res.*, 66, 4308.

Kundu, M. R., Gergely, T. E., Szabo, A., Loiacono, R., and White, S. M. 1986, *Ap. J.*, 308, 436.

Lin, R. P., Schwartz, R. A., Kane, S. R., Pelling, R. M., and Hurley, K. C. 1984, *Ap. J.*, 283, 421.

Thejappa, G., Gopalswamy, N., and Kundu, M. R. 1990, *Solar Phys.*, 127, 165.

White, S. M., Kundu, M. R., and Szabo, A. 1986, *Solar Phys.*, 107, 135.

Zheleznyakov, V. V., and Zlotnik, E. Ya. 1964, *Sov. Astron.-AJ*, 7, 485.

TABLE I
Observed Properties of a Sample of 1.4 GHz Microbursts

Event ID	Time (IAT)	Active Region	θ ($''$)	S_{max} (sfu)	τ (sec)	Deg. Pol'n	α
1	18:52:40	5689	34	3.5	20	31% LCP	-3.1
2	18:54:10	5689	30	4	30	33% LCP	-3.1
3	18:56:40	5689	30	3.8	20	31% LCP	-3.3
4	19:09:50	5676	32	0.7	20	100% RCP	8.2
5	19:10:20	5676	30	0.7	40	100% RCP	4.3
6	19:30:10	5683	26	0.18	30	100% RCP	2.2
7	19:33:40	5683	22	0.24	20	100% RCP	-4.9
8	19:35:00	5683	24	0.38	30	100% RCP	2.9
9	19:55:00	5680	15	0.07	40	100% RCP	8
10	19:55:10	5683	17	0.45	20	0-20% RCP	-2.2
11	20:05:50	5683	29	0.18	10	100% RCP	30

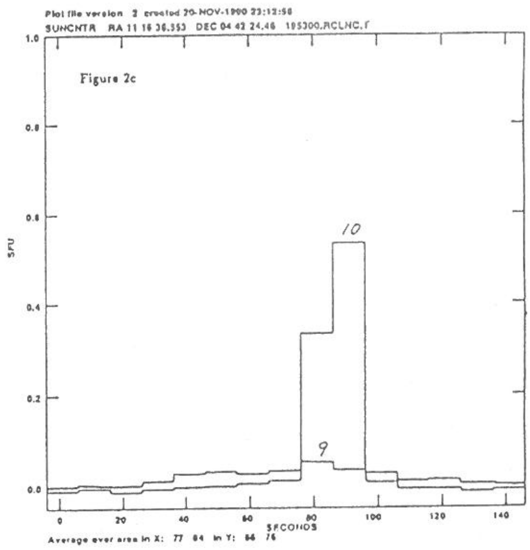

Figure 2c

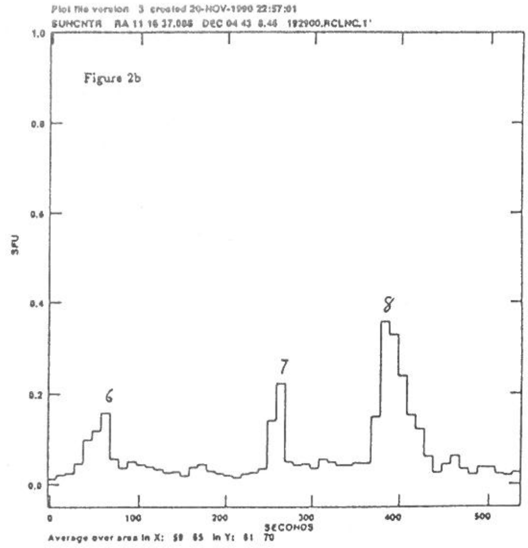

Figure 2b

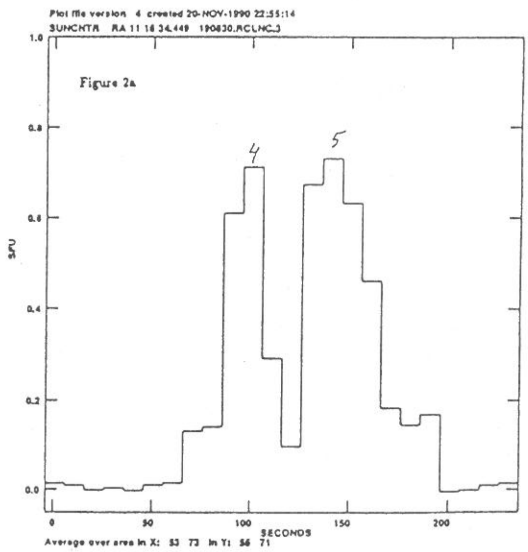

Figure 2a

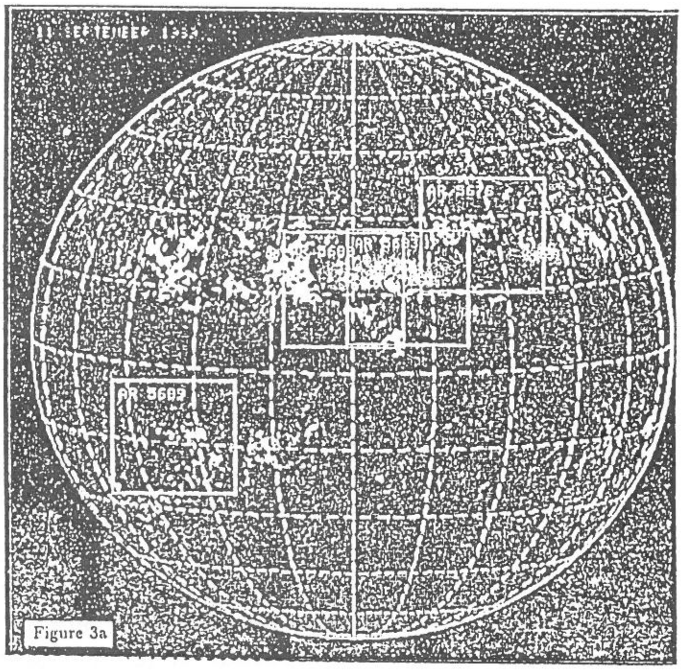

Figure 3a

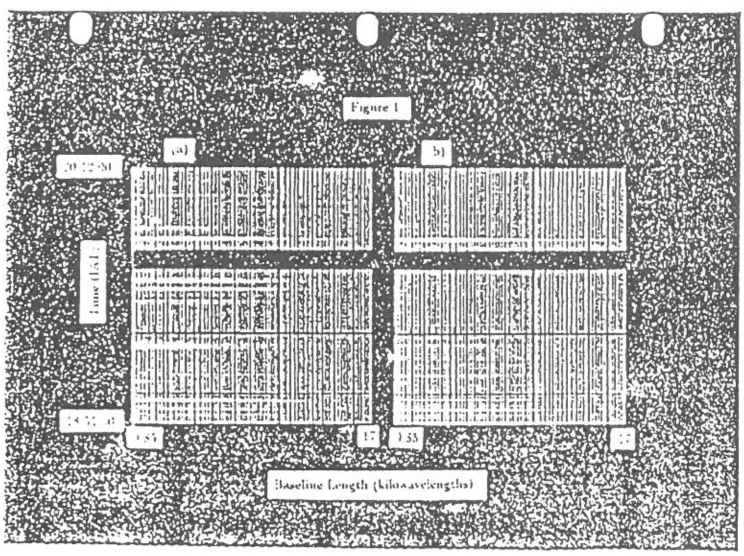

Figure 1